An active hybrid plasmonic metamaterial

Jianqiang Gu,[1,2] Ranjan Singh,[2,3] Abul. K. Azad,[3] Jiaguang Han,[1] Antoinette J. Taylor,[3] John F. O'Hara,[2,3] and Weili Zhang[1,2,*]

[1]*Center for Terahertz waves and College of Precision Instrument and Optoelectronics Engineering, Tianjin University, and the Key Laboratory of Optoelectronics Information and Technology (Ministry of Education), Tianjin 300072, China*

[2]*School of Electrical and Computer Engineering, Oklahoma State University, Stillwater, Oklahoma 74078, USA*

[3]*Center for Integrated Nanotechnologies, Materials Physics and Applications Division, Los Alamos National Laboratory, Los Alamos, New Mexico 87545, USA*

**weili.zhang@okstate.edu*

Abstract: We demonstrate an engineered composite film that dynamically switches resonant transmission behavior of terahertz radiation from band-stop to band-pass under appropriate optical pumping. In the absence of pumping, a resonant band-stop behavior is observed arising from metallic split-ring-resonators fabricated on an epitaxial silicon film that was already patterned into a periodic hole-array. Pumping with external infrared light, the silicon film becomes quasi-metallic, damping the planar metamaterial response and enabling a band-pass surface-plasmon resonance through the now conducting hole array. By leveraging two separate types of electromagnetic behaviors simultaneously, this composite chip paves a way for developing unique hybrid planar metamaterials.

OCIS codes: (160.3918) Metamaterials; (240.6680) Surface plasmons.

References and links

1. H. T. Chen, W. J. Padilla, J. M. O. Zide, A. C. Gossard, A. J. Taylor, and R. D. Averitt, "Active terahertz metamaterial devices," Nature **444**(7119), 597–600 (2006).
2. O. Paul, C. Imhof, B. Lägel, S. Wolff, J. Heinrich, S. Höfling, A. Forchel, R. Zengerle, R. Beigang, and M. Rahm, "Polarization-independent active metamaterial for high-frequency terahertz modulation," Opt. Express **17**(2), 819–827 (2009).
3. H. T. Chen, J. F. O'Hara, A. K. Azad, A. J. Taylor, R. D. Averitt, D. B. Shrekenhamer, and W. J. Padilla, "Experimental demonstration of frequency-agile terahertz metamaterials," Nat. Photonics **2**(5), 295–298 (2008).
4. W. J. Padilla, A. J. Taylor, C. Highstrete, M. Lee, and R. D. Averitt, "Dynamical electric and magnetic metamaterial response at terahertz frequencies," Phys. Rev. Lett. **96**(10), 107401 (2006).
5. N.-H. Shen, M. Massaouti, M. Gokkavas, J.-M. Manceau, E. Ozbay, M. Kafesaki, T. Koschny, S. Tzortzakis, and C. M. Soukoulis, "Optically implemented broadband blueshift switch in the terahertz regime," Phys. Rev. Lett. **106**(3), 037403 (2011).
6. Z. Tian, R. Singh, J. Han, J. Gu, Q. Xing, J. Wu, and W. Zhang, "Terahertz superconducting plasmonic hole array," Opt. Lett. **35**(21), 3586–3588 (2010).
7. H. Tao, A. C. Strikwerda, K. Fan, W. J. Padilla, X. Zhang, and R. D. Averitt, "Reconfigurable terahertz metamaterials," Phys. Rev. Lett. **103**(14), 147401 (2009).
8. R. Singh, E. Plum, W. Zhang, and N. I. Zheludev, "Highly tunable optical activity in planar achiral terahertz metamaterials," Opt. Express **18**(13), 13425–13430 (2010).
9. T. Driscoll, H.-T. Kim, B.-G. Chae, B.-J. Kim, Y.-W. Lee, N. M. Jokerst, S. Palit, D. R. Smith, M. Di Ventra, and D. N. Basov, "Memory metamaterials," Science **325**(5947), 1518–1521 (2009).
10. J. Han and A. Lakhtakia, "Semiconductor split-ring resonators for thermally tunable terahertz metamaterials," J. Mod. Opt. **56**(4), 554–557 (2009).
11. J. Gu, R. Singh, Z. Tian, W. Cao, Q. Xing, M. He, J. W. Zhang, J. Han, H.-T. Chen, and W. Zhang, "Terahertz superconductor metamaterial," Appl. Phys. Lett. **97**(7), 071102 (2010).
12. R. Singh, I. A. I. Al-Naib, Y. Yang, D. Roy Chowdhury, W. Cao, C. Rockstuhl, T. Ozaki, R. Morandotti, and W. Zhang, "Observing metamaterial induced transparency in individual Fano resonators with broken symmetry," Appl. Phys. Lett. **99**(20), 201107 (2011).
13. H. T. Chen, H. Yang, R. Singh, J. F. O'Hara, A. K. Azad, S. A. Trugman, Q. X. Jia, and A. J. Taylor, "Tuning the resonance in high-temperature superconducting terahertz metamaterials," Phys. Rev. Lett. **105**(24), 247402 (2010).
14. B. B. Jin, C. H. Zhang, S. Engelbrecht, A. Pimenov, J. B. Wu, Q. Y. Xu, C. H. Cao, J. Chen, W. W. Xu, L. Kang, and P. H. Wu, "Low loss and magnetic field-tunable superconducting terahertz metamaterial," Opt. Express **18**(16), 17504–17509 (2010).

#158013 - $15.00 USD Received 14 Nov 2011; revised 28 Nov 2011; accepted 28 Nov 2011; published 1 Dec 2011

15. R. Singh, A. K. Azad, Q. X. Jia, A. J. Taylor, and H. T. Chen, "Thermal tunability in terahertz metamaterials fabricated on strontium titanate single-crystal substrates," Opt. Lett. **36**(7), 1230–1232 (2011).
16. S. Linden, C. Enkrich, M. Wegener, J. Zhou, T. Koschny, and C. M. Soukoulis, "Magnetic response of metamaterials at 100 terahertz," Science **306**(5700), 1351–1353 (2004).
17. A. K. Azad, J. Dai, and W. Zhang, "Transmission properties of terahertz pulses through subwavelength double split-ring resonators," Opt. Lett. **31**(5), 634–636 (2006).
18. R. Singh, I. A. I. Al-Naib, M. Koch, and W. Zhang, "Sharp Fano resonances in THz metamaterials," Opt. Express **19**(7), 6312–6319 (2011).
19. S. Xiao, L. Liu, and M. Qiu, "Resonator channel drop filters in a plasmon-polaritons metal," Opt. Express **14**(7), 2932–2937 (2006).
20. S. Fan, P. R. Villeneuve, J. D. Joannopoulos, and H. Haus, "Channel drop filters in photonic crystals," Opt. Express **3**(1), 4–11 (1998).
21. T. W. Ebbesen, H. J. Lezec, H. F. Ghaemi, T. Thio, and P. A. Wolff, "Extraordinary optical transmission throughsub-wavelength hole arrays," Nature **391**(6668), 667–669 (1998).
22. R. Gordon, A. G. Brolo, A. McKinnon, A. Rajora, B. Leathem, and K. L. Kavanagh, "Strong polarization in the optical transmission through elliptical nanohole arrays," Phys. Rev. Lett. **92**(3), 037401 (2004).
23. W. Zhang, "Resonant terahertz transmission in plasmonic arrays of subwavelength holes," Eur. Phys. J. Appl. Phys. **43**(1), 1–18 (2008).
24. D. Qu, D. Grischkowsky, and W. Zhang, "Terahertz transmission properties of thin, subwavelength metallic hole arrays," Opt. Lett. **29**(8), 896–898 (2004).
25. J. Gómez Rivas, C. Schotsch, P. Haring Bolivar, and H. Kurz "Enhanced transmission of THz radiation through subwavelength holes," Phys. Rev. B **68**(20), 201306 (2003).
26. M. A. Noginov, G. Zhu, A. M. Belgrave, R. Bakker, V. M. Shalaev, E. E. Narimanov, S. Stout, E. Herz, T. Suteewong, and U. Wiesner, "Demonstration of a spaser-based nanolaser," Nature **460**(7259), 1110–1112 (2009).
27. J. N. Anker, W. P. Hall, O. Lyandres, N. C. Shah, J. Zhao, and R. P. Van Duyne, "Biosensing with plasmonic nanosensors," Nat. Mater. **7**(6), 442–453 (2008).
28. J. F. O'Hara, R. Singh, I. Brener, E. Smirnova, J. Han, A. J. Taylor, and W. Zhang, "Thin-film sensing with planar terahertz metamaterials: sensitivity and limitations," Opt. Express **16**(3), 1786–1795 (2008).
29. W. Zhang, A. K. Azad, J. Han, J. Xu, J. Chen, and X. C. Zhang, "Direct observation of a transition of a surface plasmon resonance from a photonic crystal effect," Phys. Rev. Lett. **98**(18), 183901 (2007).
30. Z. Tian, A. K. Azad, X. Lu, J. Gu, J. Han, Q. Xing, A. J. Taylor, J. F. O'Hara, and W. Zhang, "Large dynamic resonance transition between surface plasmon and localized surface plasmon modes," Opt. Express **18**(12), 12482–12488 (2010).
31. R. Singh, C. Rockstuhl, and W. Zhang, "Strong influence of packing density in terahertz metamaterials," Appl. Phys. Lett. **97**(24), 241108 (2010).
32. K. P. H. Lui and F. A. Hegmann, "Ultrafast carrier relaxation in radiation-damaged silicon-on-sapphire studied by optical-pump-terahertz-probe experiments," Appl. Phys. Lett. **78**(22), 3478–3480 (2001).
33. R. Singh, E. Smirnova, A. J. Taylor, J. F. O'Hara, and W. Zhang, "Optically thin terahertz metamaterials," Opt. Express **16**(9), 6537–6543 (2008).
34. R. Singh, A. K. Azad, J. F. O'Hara, A. J. Taylor, and W. Zhang, "Effect of metal permittivity on resonant properties of terahertz metamaterials," Opt. Lett. **33**(13), 1506–1508 (2008).
35. D. Grischkowsky, S. Keiding, M. Exter, and C. Fattinger, "Far-infrared time-domain spectroscopy with terahertz beams of dielectrics and semiconductors," J. Opt. Soc. Am. B **7**(10), 2006–2015 (1990).

1. Introduction

There has been intense focus on developing active metamaterial (MM) devices in the terahertz regime where a lack of suitable natural materials has created a longstanding technology gap. The MM paradigm can bridge this gap by enabling materials with customized and even dynamic electromagnetic responses. Recently, characteristic control of terahertz waves was demonstrated using active MM devices controlled through electronic, optical, mechanical, and thermal means [1–15]. Usually, active control is employed to alter the fundamental resonance of the split-ring-resonator (SRR) structure, which natively exhibits a band-stop behavior in the transmission spectra [16–18]. However, if this band stop mode could be dynamically switched to a band-pass resonance at the same frequency, the resulting MMs could be promising in active terahertz applications, such as channel-drop filtering or frequency shift keying [19,20].

Surface plasmon polaritons (SPPs) are the electromagnetic surface waves that result from the coupling of incident light to the collective oscillations of free electrons at a metal-dielectric interface [21–25]. SPPs have shown the potential to unify photonics and electronics resulting in the exciting field of plasmonics. This has led to the development of an entirely new class of miniaturized lasers [26] and biosensing devices [27,28]. More fundamentally, SPPs can resonantly intensify the transmission of electromagnetic energy through subwavelength hole arrays in metallic films, a phenomenon known as extraordinary

#158013 - $15.00 USD Received 14 Nov 2011; revised 28 Nov 2011; accepted 28 Nov 2011; published 1 Dec 2011

transmission. As both MMs and SPPs offer unique and powerful methods to resonantly control electromagnetic waves, they are being evaluated for use in electronic and photonic circuitry to better manipulate electromagnetic waves and for their feasibility of integration into large scale manufacturing of microprocessors and computer chips. So far, however, there are no reports on the development of terahertz devices in which both the metamaterial SRR resonance and the resonant propagation of SPPs could operate actively with external pumping by photons in order to enable a new type of dynamic material response.

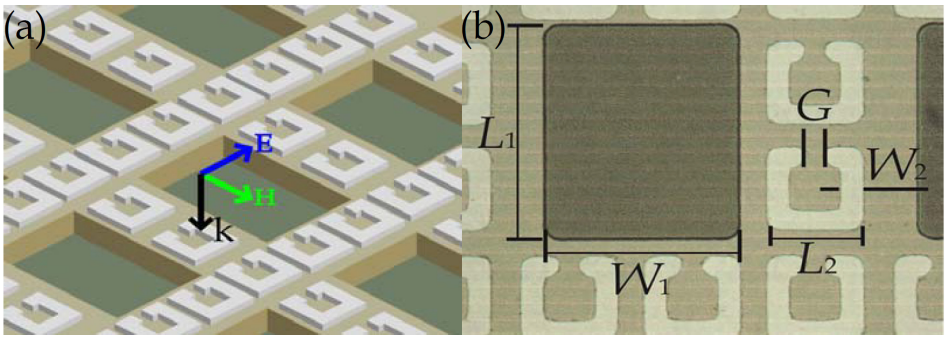

Fig. 1. (a) Schematic and (b) microscopic image of the plasmonic MM (silicon, aluminum and sapphire are marked by yellow, white and green colors, respectively). The geometrical dimensions of the MM are L_1 = 65 μm, W_1 = 50 μm, L_2 = 33 μm, W_2 = 6 μm, and G = 5 μm.).

In this article, we present a composite plasmonic two-dimensional (planar) MM with a resonant transmission that can be dynamically tuned between band-stop or band-pass behaviors by illuminating the device with near infrared light. The fundamental SRR resonance of the MM enables a band-stop behavior while the resonant extraordinary transmission due to SPPs enables a band-pass behavior. This unique functionality is achieved by integrating the metallic SRRs together with a hole array patterned into the silicon film of a silicon-on-sapphire substrate (SOS). The carrier concentration in silicon can be dynamically tuned by pumping it with a near infrared light, a property that can be exploited to tune the resonance of devices fabricated on SOS [29,30]. The silicon layer gradually becomes quasi-metallic under increasing near infrared illumination due to the excitation of free carriers. This effectively shorts the capacitive gaps and damps the SRR resonance, and destroys the band-stop terahertz response. The silicon hole arrays, if sufficiently conducting, have the capability to support the propagation of surface waves as reported in previous works [29,30]. Therefore, the high infrared fluence simultaneously enables the formation of an SPP resonance resulting in a well-defined transmission peak in the terahertz spectrum. Our supporting numerical simulations agree well with the experimentally measured results and illustrate the characteristic switching from the MM resonance to the extraordinary SPP transmission by visualizing the electric field distributions at the resonance frequency.

2. Planar metamaterial structure design and fabrication

The plasmonic planar MM sample was fabricated on a 350 μm thick SOS wafer with a 500 nm thick, undoped epitaxial silicon layer. The conductivity of the silicon layer has been shown to be tunable from 10^3 to 10^5 S/m by an 800 nm optical pump with fluence ranging from 100 to 1000 μJ/cm^2 [29]. This changes the silicon from a good dielectric to a film with some degree of metallic character. Thus, without the optical pump the planar MM is mainly an SRR array sitting on a dielectric substrate. Some resonance strength is sacrificed by the sparser than usual arrangement of SRRs [31]. When the conductivity of the silicon layer is dynamically increased up to 10^4 S/m, all the SRRs fabricated on the silicon layer are shorted out due to the flow of current in their capacitive gaps. Moreover, the metallic silicon hole array starts to support SPPs leading to enhanced transmission, in which the resonance frequency ω_{SP} of the SPPs is determined by $\omega_{SP}/2\pi = (c/p)\left[\varepsilon_{Si}\varepsilon_{sphr}/\left(\varepsilon_{Si}+\varepsilon_{sphr}\right)\right]^{-1/2}$, where

#158013 - $15.00 USD Received 14 Nov 2011; revised 28 Nov 2011; accepted 28 Nov 2011; published 1 Dec 2011

c is the speed of light in vacuum, p is the periodicity of the hole in the direction of the incident electric field, $\varepsilon_{sphr} = 11.7$ is the permittivity of the sapphire substrate and ε_{Si} is the permittivity of the photo-excited silicon layer, which may reach as low as ~-90 through photodoping under intense optical excitation [24,29].

Figure 1 shows the schematic and a microscopic image of the fabricated structure. The aluminum SRR array was patterned on the silicon film by using a conventional photolithography process. This was followed by reactive ion etching to form the hole array in the silicon film. Five SRRs and a silicon hole, with dimensions of 33 × 33 μm^2 and 65 × 50 μm^2 respectively, comprise each of the unit cells, as shown in Fig. 1(a), which have a periodicity of 100 × 100 μm^2. With this periodicity, the SPP resonance for the silicon-sapphire interface occurs near 0.5~1 THz, while the air-silicon SPP resonance frequency occurs near 3 THz, which is beyond our measurement range. This means these two SPP resonances will not interact with each other though the fully pumped silicon has a ~1 μm skin depth that is larger than the silicon thickness. The gap-bearing arm of the SRR was designed to be parallel with the width of the holes. These dimensions and orientations of the SRRs and holes were designed such that the fundamental SRR resonance and the [1,0] SPP resonance occur at the same frequency.

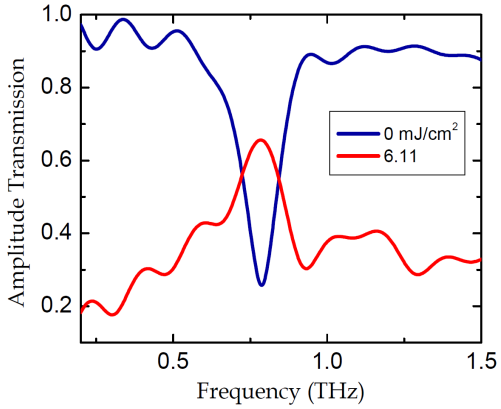

Fig. 2. Simulated amplitude transmission with no pump and with maximum pump fluence 6.11 mJ/cm^2.

Figure 2 shows the full-wave electromagnetic simulation carried out by CST Microwave Studio for two extreme cases, first assuming that the silicon acts as a insulator (i.e. no external pumping) having a dielectric constant of 11.78, and second when the silicon layer acts as a lossy metal (i.e. at maximum optical pump power in the experimental system) with a conductivity of 2.94 × 10^5 S/m. An exact match of the planar MM and the SPP resonances was satisfied at a single frequency of 0.8 THz, as shown in Fig. 2. This simulation guided the structural design of the SRRs and the holes in the plasmonic planar MM before sample fabrication.

#158013 - $15.00 USD Received 14 Nov 2011; revised 28 Nov 2011; accepted 28 Nov 2011; published 1 Dec 2011

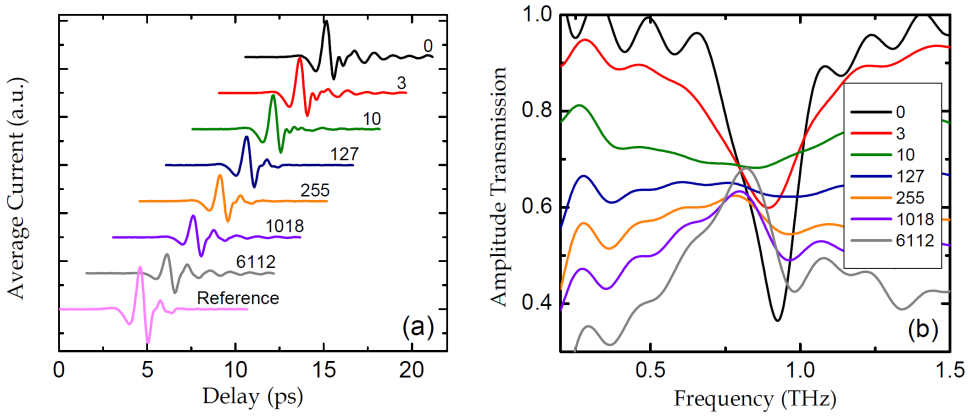

Fig. 3. Measured (a) time-domain terahertz pulses and (b) transmission spectra at different pump fluences (μJ/cm^2).

3. Transmission results and analysis

The sample was characterized using an electro-optic, time-resolved optical–pump terahertz–probe (OPTP) spectrometer [29]. The OPTP system utilizes a regenerative Ti:Sapphire amplifier that delivers 3.2 mJ, 50 fs laser pulses at 800 nm with a 1 kHz repetition rate. The output laser beam is split into two parts with one being used for terahertz generation-detection and the other for optical excitation of the sample through a variable attenuator. The linearly polarized terahertz beam is transmitted through the sample under normal incidence with the terahertz electric field parallel to the gap bearing arm of the SRRs. The optical beam, with spot size (1x1 cm^2) larger than the terahertz spot (5x5 mm^2), provides mostly uniform excitation over the measurement area. A bare SOS wafer serves as a reference by which terahertz transmission measurements are normalized.

Figure 3(a) shows the transmitted terahertz pulses through the composite plasmonic film at various pump fluences. By visual inspection the measured terahertz pulses can be categorized into three groups based on the ringing that occurs after the main terahertz pulses. Without optical excitation the terahertz pulse shows a long-lived ringing which is due to the SRR fundamental resonance. Under low optical excitation this ringing gradually fades away with increasing power suggesting a weakening of the SRR resonances. While excited with a moderate optical fluence (10-255 μJ/cm^2), the shape of the pulse is nearly the same as the reference signal but with lower amplitude suggesting the disappearance of the SRR resonance. Finally, when the power is increased beyond 255 μJ/cm^2, the ringing in the pulse is restored but the nature of oscillation appears to be different from the optically unexcited sample. The dynamic change in nature of the oscillations indicates a corresponding modulation in transmission as verified in Fig. 3(b), which is the Fourier transform of the measured time domain pulses. The spectrum for the unpumped sample shows the strongest SRR resonance with band-stop transmission amplitude as low as 0.36. When the excitation fluence is gradually increased from 0 to 10 μJ/cm^2, the SRR resonance disappears and the transmission amplitude increases from 0.36 to 0.7. Under 10 μJ/cm^2 excitation the SRR resonance completely disappears and the transmission spectrum shows a flat attenuation. Further increase of the optical fluence up to 255 μJ/cm^2 only reduces the flat amplitude transmission from 0.68 to 0.62 due to increasing photo-carriers in the silicon layer. As the fluence is increased above 255 μJ/cm^2, a resonance peak appears in the transmission spectrum whose amplitude increases with excitation power. The measured peak is attributed to the SPP resonance excited by the semi-metallic silicon hole arrays.

#158013 - $15.00 USD Received 14 Nov 2011; revised 28 Nov 2011; accepted 28 Nov 2011; published 1 Dec 2011

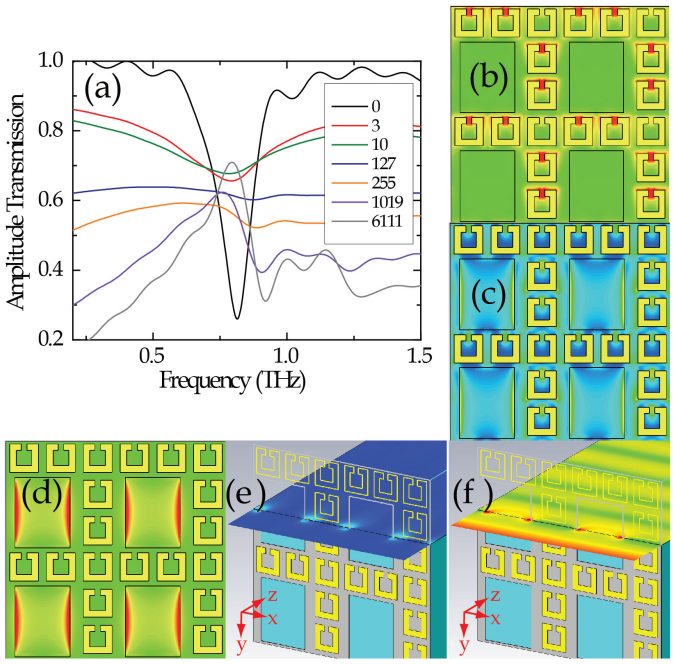

Fig. 4. (a) Simulated spectra at different pump fluences. Simulated electric fields at different pump fluencies (μJ/cm^2): (b) no pump, (c) 127 μJ/cm^2, (d) 6.11 mJ/cm^2, (e) and (f) Ex and Ez distribution at 6.11 mJ/cm^2.

In order to gain insight into the pump-dependent behavior of the plasmonic planar MM, we performed full wave electromagnetic simulations (CST Microwave Studio) of terahertz transmission through the sample with periodic boundary condition and plane wave incidence. Since the tunable response arises from the change in conductivity of the silicon layer, we employed different conductivities in the numerical simulation to represent different pump powers [3,32]. The simulated amplitude transmissions are shown in Fig. 4(a) which agrees well with the measurements. The electric field distributions at the resonance frequency were simulated for three different conductivities of 0 (no pump), 7.6×10^3 (127 μJ/cm^2), and 2.94×10^5 S/m (6112 μJ/cm^2), as shown in Figs. 4(b)–4(d), respectively. We clearly observe the transition from high concentration of electric field in the SRR gaps with no pump to intense fields at the edge of the hole arrays with maximum pumping. At the maximum pump fluence the conductivity of the silicon film is high enough to support a SPP resonance. At this pump level the metal SRRs are effectively shorted against the metallic silicon film. The hole array builds up a strong SPP band-pass transmission resonance wherein the electric field is mainly focused along the length of the holes. To confirm the SPP mechanism, the distributions of the electric field components parallel to the width of the hole (Ex) and parallel to the propagation direction (Ez) were plotted in Figs. 4(e) and 4(f) at 6.11 mJ/cm^2, respectively. The strong intensity of Ez obviously verifies the collection of the charges at the long sides of the hole, which is a typical SPP phenomenon. Interestingly, for moderate pump fluences neither the SRR nor the SPP resonance feature was observed in Fig. 4(c) since the electric field appears to be fairly uniform across the entire sample. The reason is that the conductivity of the silicon layer was enough to damp the SRR resonance but not enough to support the propagation of surface waves, which normally requires some minimum threshold of both metal conductivity and thickness [33,34].

4. Discussion

As shown in Figs. 3(b) and 4(a), the quality factors of the SRR and the SPP resonances are not as high as expected. Most of this is due to the large coupling between the resonant modes and

#158013 - $15.00 USD Received 14 Nov 2011; revised 28 Nov 2011; accepted 28 Nov 2011; published 1 Dec 2011

freely propagating waves, which is often expressed in the concept of large radiation resistance. However, our structure also has other dissipation mechanisms that limit the intensity and the linewidth of the resonances. The source of dissipation in our device is Ohmic loss in either the metal SRRs for the resonance, or the photoexcited Si for the SPP resonance. The sapphire losses are small enough to neglect in the terahertz regime [35]. The relatively sparse arrangement of SRRs also reduces the resonance intensity. Generally, for most planar metamaterials and plasmonics devices the dissipation cannot be overcome without the use of a gain medium. But for our planar metamaterial, the dissipation is acceptable, in contrast to bulk metamaterials, because its functionality is contained in a single layer.

The measured results demonstrate the most straightforward manifestation of switching between two resonant responses of different natures. However, the concept can easily be extended to more interesting electromagnetic scenarios. Since SRRs are both electrically and magnetically polarizable, *s*-polarized, obliquely incident waves should be able to excite the fundamental SRR resonance of the SRR array via the magnetic field. Given the nature of SPP coupling in periodic arrays, it also remains possible to launch the SPPs, though the SPP resonance would occur at a different frequency due to phase matching conditions. However, it is possible to resize the SRRs and frequency shift their resonance into alignment with the oblique SPP resonance. Upon optical stimulation, the resulting structure would dynamically shift from a magnetic bandstop filter to an electric bandpass filter. This ultrafast dynamic control over the dynamic bianisotropic properties is under investigation and represents a new and relatively unexplored area of metamaterial research.

5. Conclusion

We have developed a MM embedded plasmonic device that enables dynamic switching between two separate types of electromagnetic behaviors, i.e. the SRR and SPP resonance modes. The plasmonic planar MM allows a giant modulation at the resonance frequency, altering from the band-stop mode to the band-pass mode. This feature is due to the tunable conductivity of a silicon thin film under photo excitation. Such active control of different resonances offers a unique tool at the MM designers' disposal and is promising in developing on-chip terahertz devices in microchip circuitry, such as dynamic channel add/drop filters. In addition, this work heralds a possible approach to ultrafast dynamic control over bianisotropic metamaterial properties.

Acknowledgments

This work was supported by the National Science Foundation of China (Grant Nos. 61138001, 61028011, 61007034, and 61107053) and the U.S. National Science Foundation. The Los Alamos team gratefully acknowledges the LDRD Program and the Center for Integrated Nanotechnologies for partially supporting this work.

#158013 - $15.00 USD Received 14 Nov 2011; revised 28 Nov 2011; accepted 28 Nov 2011; published 1 Dec 2011